

AD-A041 047

ATLANTIC RESEARCH CORP ALEXANDRIA VA
INVESTIGATION OF PG/SIC PROCESSING VARIABLES.(U)
MAR 77 J P COPELAND, C W NEWQUIST

F/G 11/3

F33615-74-C-5098

UNCLASSIFIED

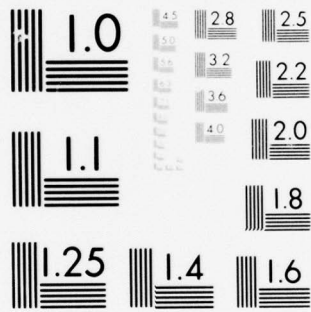
AFML-TR-76-123

NL

1 OF 1

AD
A041047





MICROCOPY RESOLUTION TEST CHART
NATIONAL BUREAU OF STANDARDS-1963-A

AD A041047

AFML-TR-76-123

12
NW

INVESTIGATION OF PG/SiC PROCESSING VARIABLES

ATLANTIC RESEARCH CORPORATION
5390 CHEROKEE AVENUE
ALEXANDRIA, VIRGINIA 22314

MARCH 1977

TECHNICAL REPORT AFML-TR-76-123
FINAL REPORT FOR PERIOD 1 APRIL 1974 - 1 OCTOBER 1975

Approved for public release; distribution unlimited

AU NO. _____
DDC FILE COPY

AIR FORCE MATERIALS LABORATORY
SPACE AND MISSILES SYSTEMS BRANCH
SYSTEMS SUPPORT DIVISION
WRIGHT-PATTERSON AIR FORCE BASE, OHIO 45433


DDC
RECEIVED
JUN 27 1977
D

NOTICE

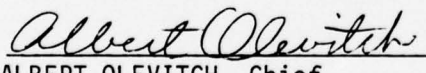
When Government drawings, specifications, or other data are used for any purpose other than in connection with a definitely related Government procurement operation, the United States Government thereby incurs no responsibility nor any obligation whatsoever; and the fact that the government may have formulated, furnished, or in any way supplied the said drawings, specifications, or other data, is not to be regarded by implication or otherwise as in any manner licensing the holder or any other person or corporation, or conveying any rights or permission to manufacture, use, or sell any patented invention that may in any way be related thereto.

This final technical report was submitted by Atlantic Research Corporation, 5390 Cherokee Avenue, Alexandria, Virginia 22314 under Contract F33615-74-C-5098, Job Order No. 73500214 with the Air Force Materials Laboratory, Wright-Patterson Air Force Base, Ohio 45433. Mr. John D. Latva, AFML/MXS, was the laboratory project monitor.

This technical report has been reviewed and is approved for publication.


John D. Latva
Project Engineer

FOR THE COMMANDER


ALBERT OLEVITCH, Chief
Non-Metals Engineering Branch
Systems Support Division
AF Materials Laboratory
Copies of this report should not be returned unless return is required by security considerations, contractual obligations, or notice on a specific document.

UNCLASSIFIED

SECURITY CLASSIFICATION OF THIS PAGE (When Data Entered)

REPORT DOCUMENTATION PAGE		READ INSTRUCTIONS BEFORE COMPLETING FORM
1. REPORT NUMBER AFML-TR-76-123	2. GOVT ACCESSION NO.	3. RECIPIENT'S CATALOG NUMBER
4. TITLE (and Subtitle) Investigation of PG/SiC Processing Variables	5. TYPE OF REPORT & PERIOD COVERED Final 1 April 1974-1 October 1974	
6. AUTHOR(s) J. P. Copeland, C. W. Newquist, R. S. Valentine	7. CONTRACT OR GRANT NUMBER(s) F33615-74-C-5098	
9. PERFORMING ORGANIZATION NAME AND ADDRESS Atlantic Research Corporation 5390 Cherokee Avenue Alexandria, VA 22314	10. PROGRAM ELEMENT, PROJECT, TASK AREA & WORK UNIT NUMBERS 7340/734001/3059	
11. CONTROLLING OFFICE NAME AND ADDRESS Air Force Materials Laboratory Wright-Patterson Air Force Base, Ohio 45433	12. REPORT DATE 30 March 1977	
14. MONITORING AGENCY NAME & ADDRESS (if different from Controlling Office)	13. NUMBER OF PAGES 53	
	15. SECURITY CLASS. (of this report) UNCLASSIFIED	
16. DISTRIBUTION STATEMENT (of this Report) Approved for public release; distribution is unlimited.		
17. DISTRIBUTION STATEMENT (of the abstract entered in Block 20, if different from Report)		
18. SUPPLEMENTARY NOTES		
19. KEY WORDS (Continue on reverse side if necessary and identify by block number) chemical vapor deposition reduced pressure codeposition codeposits pyrolytic graphite silicon carbide alloyed pyrolytic graphite		
20. ABSTRACT (Continue on reverse side if necessary and identify by block number) This report describes a program conducted to investigate the relationships between process conditions and Pg/SiC codeposit coating characteristics. The work was directed primarily toward the investigation of conditions other than those routinely used to coat test components for other programs. The program involved two areas of study: (1) reduced (subatmospheric) pressure codeposition and (2) gas flow characteristics in atmospheric pressure furnaces used to coat large nozzle components.		

UNCLASSIFIED

SECURITY CLASSIFICATION OF THIS PAGE(When Data Entered)

20. >The deposition study involved the conduct of a series of experimental runs in order to establish conditions which produced an acicular SiC structure in the codeposit. Then a final run was conducted in an attempt to apply a coating with this microstructure to a contoured surface which simulated a subscale nose cap.

The flow study involved the construction and operation of a 2D water analog of large deposition furnaces. The analog was used to simulate flow patterns in furnace assemblies then in use to coat nose caps and throat inserts for 7.0 inch nozzles.

A major conclusion of this program is that the SiC structure is dependent upon pressure, but an acicular SiC structure can be achieved at reduced pressure. Further, acceptable deposition rates can be achieved at reduced pressure. Generally, smooth coatings result and the bond with the substrate material (ATJ graphite) is strong. ←

UNCLASSIFIED

SECURITY CLASSIFICATION OF THIS PAGE(When Data Entered)

PREFACE

This technical report was prepared in partial fulfillment of the requirements of Contract F33615-74-C-5098, AFML Project No. 7340 Task No. 734001 and AFRPL Project No. 3059 with the Space and Missiles Systems Branch, Systems Support Division, Air Force Materials Laboratory. Lt. Glenn Hollenberg and Mr. John D. Latva, AFML/MXS, provided technical direction for the Air Force Materials Laboratory.

This report covers work conducted during the period 1 April 1974 through 1 October 1975 and constitutes the final report under this contract.

This study was conducted within the Nozzle Development Department, Research and Technology Division, Atlantic Research Corporation, 5390 Cherokee Avenue, Alexandria, Virginia 22314. The Principal Investigator was Dr. J. P. Copeland. Dr. R. S. Diefendorf of Rensselaer Polytechnic Institute served as Technical Consultant.

ACCESSION for	
NTIS	White Section <input checked="" type="checkbox"/>
OCB	Buff Section <input type="checkbox"/>
UNANNOUNCED	<input type="checkbox"/>
JUSTIFICATION.....	
BY.....	
DISTRIBUTION/AVAILABILITY CODES	
Dist.	AVAIL. and/or SPECIAL
A	

DDC
RECEIVED
JUN 27 1977
D

TABLE OF CONTENTS

	<u>PAGE</u>
I. INTRODUCTION	1
II. SUMMARY.	3
III. DEPOSITION STUDY	4
1. Objective.	4
2. Apparatus.	5
a. Furnaces	5
b. Temperature Measurement.	5
c. Process Gas Supply and Measurement	5
3. Parametric Deposition Experiments.	6
a. Run # 18-14: Description and Results.	6
b. Run # 18-15.	11
c. Run # 458-25	13
d. Results Comparison	18
4. Coating Application Test - Run # 107-17.	19
a. Furnace Preparation.	19
(1) Residual Soot Removal	19
(2) Methyltrichlorosilane Liquid Delivery System. . .	22
(3) Deposition Hardware	22
b. Run Description.	22
c. Results.	27
IV. FLOW ANALOG STUDIES.	33
1. Flow Simulator Design.	33
2. General Observations	35
3. Throat Insert Configuration.	36
4. Conventional Nose Cap Configuration.	39
5. Modified Single Annulus Nose Cap Configuration	42
6. Double Annulus Nose Cap Confituration.	42
7. Inverted Substrate Nose Cap Configuration.	46
8. Injector Criteria.	51
9. Conclusions from Flow Simulation Studies	51
V. CONCLUSIONS AND RECOMMENDATIONS.	53

LIST OF TABLES

TABLE		PAGE
1	Vacuum Deposition Run No. 18-14, Deposition Conditions.	9
2	Vacuum Deposition Run No. 18-15	12
3	Vacuum Deposition Run No. 458-25.	14
4	Deposition Run No. 458-25	17
5	Deposition Run No. 101-17	26
6	Throat Insert Configuration	38
7	Conventional Nosecap Configuration.	41
8	Modified Single Annulus Nosecap Configuration	44
9	Double Annulus Nosecap Configuration.	47
10	Inverted Nosecap Configuration.	50

FIGURE	LIST OF FIGURES	PAGE
1	MTS Rotameter Calibration Curve	7
2	14 Inch Vacuum Furnace (vacuum chamber not shown)	10
3	Photomicrographs of Run 428-25 PG/SiC Depositions	16
4	14 Inch I.D. Reduced Pressure Furnace (vacuum chamber not shown)	21
5	Run no. 101-17, Substrate and Support Assembly - Side View . . .	23
6	Run No. 101-17, Substrate and Support Assembly - Top View. . . .	24
7	Run No. 101-17, Substrate and Support Assembly - Coated.	28
8	Run No. 101-17, Process Conditions and Photomicrograph, Magnification 70X	29
9	Run No. 101-17, Cross-Section of Coated Subscale Nosecap. . . .	30
10	Flow Simulator in Double Annulus Configuration.	34
11	Internal Geometry for Throat Insert Deposition Runs	37
12	Internal Geometry for Single Annulus Nosecap Configuration. . .	40
13	Modified Single Annulus Nosecap Configuration	43
14	Double Annulus Nosecap Configuration.	45
15	Typical Dye Injection Flow Test of Double Annulus Configuration	48
16	Internal Geometry for Flow Tests of Inverted Substrate Nosecap Configuration	49

SECTION I INTRODUCTION

The objective of this program was to establish a fundamental interpretation of the codeposition of silicon carbide (SiC) and pyrolytic graphite (PG). Prior and concurrent Air Force-sponsored programs were primarily oriented toward the fabrication of nozzle components and material specimens for test firings and properties measurements. Consequently, the deposition effort during these programs was directed toward the fabrication of deliverable items.

The program described in this report provided a means for investigating the PG/SiC process in an orderly manner and allowed investigation of process conditions not routinely used in the past. When initiated, the program had four basic tasks:

- (1) Deposition Study - A series of experimental deposition runs were to be conducted in order to establish relationships between process conditions and coating microstructures. The results of these experiments were to aid in the development of a theoretical process model.
- (2) Characterization of Coatings - General properties including density, silicon carbide content and microstructure were to be evaluated for all coatings. Thermal expansion, both ab and c direction, were to be measured also on selected specimens.
- (3) Structural Model - An analysis was to be conducted, via a subcontract, which would relate the microstructure of codeposit coatings to selected thermal-mechanical properties.
- (4) Process Recommendation - The process and structural models were to be combined to form a procedure for predicting thermal-mechanical properties from process parameters.

At the onset of the program, at the suggestion of the technical monitor, it was decided to emphasize deposition at reduced pressure. Consequently, the run matrix for the deposition study was structured to determine conditions under which an acicular silicon carbide structure could be

obtained. When success was achieved with a simple axisymmetric, cylindrical geometry, then a final deposition run was conducted in an attempt to apply a coating with similar microstructure to a highly contoured surface, i.e., a subscale noscap.

The structural modeling effort originally planned during this program was deleted in order to provide resources for a furnace gas flow study. Difficulties had been encountered during the AFRPL Scale-Up Program when attempts were made to coat noscaps for 7.0 inch nozzles using the standard atmospheric pressure process. During the course of an in-house study of this process it became apparent that the gas flow field in the furnace was a critical process parameter. This conclusion led to the re-direction of the program to include a flow simulation task.

As a result of the re-direction, the fourth program task could not be accomplished since a structural model was not available. Further, the decision to coat nozzle components led to the consumption of the remaining resources of the program. Consequently, a rigorous process model could not be developed.

Section II summarizes the technical accomplishments of this program. A detailed discussion of the deposition study is contained in Section III. Section IV describes the flow simulation study. Section V lists the major conclusions and recommendations of this program.

SECTION II

SUMMARY

This report describes a program conducted to investigate the relationships between process conditions and PG/SiC codeposit coating characteristics. The work was directed primarily toward the investigation of conditions other than those routinely used to coat test components for other programs. The program involved two areas of study: (1) reduced (subatmospheric) pressure codeposition and (2) gas flow characteristics in atmospheric pressure furnaces used to coat large nozzle components.

The deposition study involved the conduct of a series of experimental runs in order to establish conditions which produced an acicular SiC structure in the codeposit. Then a final run was conducted in an attempt to apply a coating with this microstructure to a contoured surface which simulated a subscale nosecap.

The flow study involved the construction and operation of a 2D water analog of large deposition furnaces. The analog was used to simulate flow patterns in furnace assemblies then in use to coat nosecaps and throat inserts for 7.0 inch nozzles.

A major conclusion of this program is that the SiC structure is dependent on pressure, but an acicular SiC structure can be achieved at reduced pressure. Further, acceptable deposition rates can be achieved at reduced pressure. Generally, smooth coatings result and the bond with the substrate material (ATJ graphite) is strong.

SECTION III DEPOSITION STUDY

1. Objective and Approach

The objectives of the deposition study were to determine whether an acicular SiC structure could be codeposited with PG at reduced pressure, and if successful, to deposit a coating with this microstructure on a contoured surface such as a subscale nose cap. The initial attempts to achieve the desired structure involved adopting the diluent (N_2) flowrates and methane concentration routinely used to fabricate unalloyed PG at reduced pressure. Several coating runs were conducted during which various amounts of methyltrichlorosilane (MTS, precursor for SiC) were blended with the baseline gas mixture. None of these runs produced the desired structure. A second approach was tested in which the reactive gas composition (ratio of methane to MTS) used in the atmospheric pressure process was adopted as baseline, the diluent was eliminated and a series of coatings were deposited at various temperatures and pressures. The desired microstructure was obtained during this series. Selection of conditions for coating the nose cap contour were derived directly from the results of this second run series.

2. Apparatus

a. Furnaces

Two low pressure high temperature induction furnaces were used during this study. Both furnaces were heated by a 250 KW, 180 power supply. The larger of the two furnaces, referred to as the 14 inch I.D. reduced pressure coatings furnace, was used for runs # 18-14, # 18-15 and # 101-17. It has a usable vapor deposition chamber 14 inches in diameter by 18 inches high. The smaller furnace, referred to as the 8 inch I.D. reduced pressure coatings furnace, was used for run # 458-25. Its deposition chamber measures 8 inches in diameter by 16 inches high. The process gas injectors in both furnaces are equally spaced around the circumference of the bottom of the deposition chambers. The larger furnace has six injectors, the smaller has three. The injectors can be angled from near vertical to 18° from vertical so that the process gas flow pattern can be adjusted prior to a run.

Both furnaces are operated inside reduced pressure chambers to provide the necessary conditions for low pressure vapor deposition. The vacuum is provided by a 300 CFM mechanical pump, with filters and throttling valves between the chambers and the pump.

b. Temperature Measurement

The temperature of the deposition surface inside the furnace was monitored using a calibrated optical pyrometer (L & N # 8632-F) with accuracy traceable to the N.B.S. The calibration was performed by the pyrometer manufacturer. At a temperature of 3200° F the pyrometer was accurate within 2° F and at 4000° F the accuracy was $\pm 10^\circ\text{ F}$.

c. Process Gas Supply and Measurement

The process gases entering the furnace deposition chambers were composed of various combinations of nitrogen, methane and methyltrichlorosilane (CH_3SiCl_3). The nitrogen and methane were metered in the gaseous state through rotameters having an accuracy of $\pm 10\%$. The methyltrichlorosilane, abbreviated MTS, was metered by two different methods. During the first three runs (18-14, 18-15 and 458-25) the MTS flow was measured by

monitoring the weight loss of MTS liquid from the five gallon bubbler used to supply the MTS. The carrier gas used with the MTS bubbler was either nitrogen or methane diverted from the process gas flow. The carrier gas was recombined with the process gas stream after being saturated with MTS vapor. The other method of metering MTS, used for run # 101-17, was direct measurement of MTS liquid flow using a rotameter. The MTS was stored in a five (5) gallon pressure vessel which is refilled under pressure from a 55 gallon drum. The MTS was vaporized and combined with the process gas flow in a plenum heated to 180°F.

The rotameter used for MTS measurement was calibrated by discharging the MTS liquid from the rotameter into a graduated cylinder for a known period of time. The rate was determined three times at each of four different scale readings. The average actual volumetric flow rate was then computed in cc/hour for each scale reading and plotted against the indicated flow rate. (See Figure 1.) Repeatability was determined to be within 2% at the flow rate used in run # 101-17.

The process nitrogen is stored as a cryogenic liquid in a 2000 gallon dewar and is vaporized before entering the laboratory. Methane (commercial grade) is stored at room temperature in standard 1A size pressurized cylinders.

3. Parametric Deposition Experiments

The first three runs in this program (18-14, 18-15 and 458-25) were a series of deposition experiments designed to determine the necessary parameters* for depositing a specific type of coating of pyrolytic graphite alloyed with silicon carbide at reduced pressure conditions. Each run was divided into several segments so that more than one set of variables could be examined during each run. This procedure allowed the testing of eleven sets of parameters in three runs.

a. Run #18-14: Description and Results

Deposition run # 18-14 was performed in the 14 inch I.D.

*(e.g., temperature, pressure, gas flow, gas mixture)

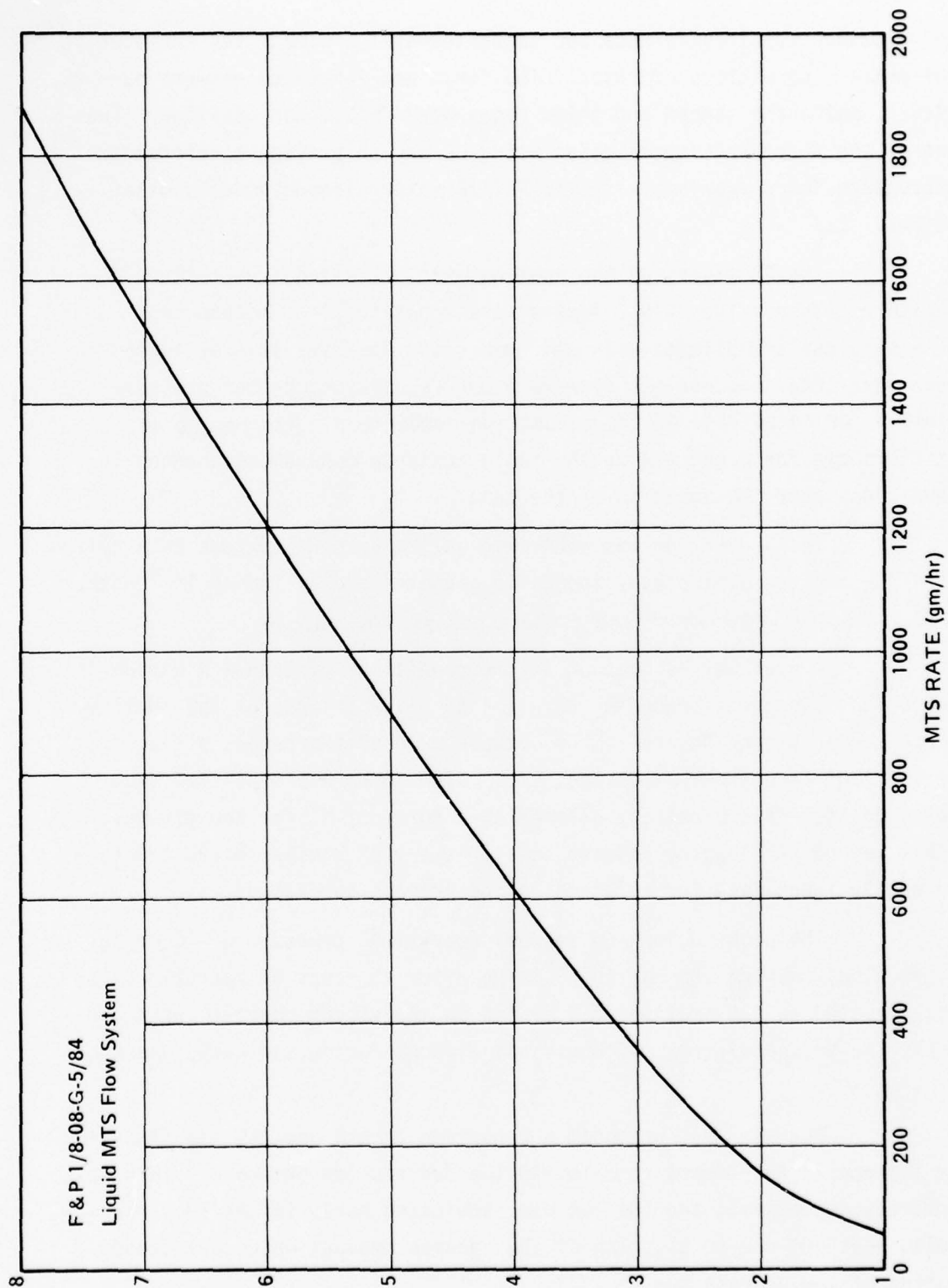


Figure 1. MTS Rotameter Calibration Curve.

reduced pressure coatings furnace and consisted of four separate, consecutive sets of process conditions or cases. The first and fourth cases were pure PG deposition, while the second and third cases were PG/SiC codeposition. The purpose of the first and fourth cases using PG was to provide a reference microstructure for comparison with the PG/SiC material made under similar conditions.

The PG layers of the coating were deposited from methane diluted with nitrogen. The PG/SiC layers were deposited from methane and methyltrichlorosilane diluted with nitrogen. The parameters investigated in this run were total process gas flow rate and deposition chamber pressure. See Table 1 for an outline of the deposition conditions. The ranges of conditions shown for each case in the table indicate continuous changes in the conditions over the duration of the case.

The deposition was performed on the outside surface of a cylindrical ATJ graphite substrate, 4 inches in diameter and 16 inches in length. Figure 2 shows the geometry of the furnace deposition chamber.

A one hour PG precoat at the conditions of Case # 1 was deposited on the substrate preceding Case # 1 to allow release of the coating. Between the precoat and Case # 1, and between each of the cases, a flag or marker layer of carbon was deposited. This flag layer was deposited from undiluted CH_4 for five minutes, followed by a purge of N_2 for ten minutes. With this method of flagging between cases, layers of similar microstructure can be easily identified for relation to the process conditions.

The planned furnace chamber operating pressure of 13 mm Hg increased slowly during the run to 53 mm Hg after 15 hours of operation. An air leak related to the heating of a flange on the vacuum chamber was responsible for the pressure rise, which was not evident during the early hours of the run.

The air leak prompted a reduction of the process gas flows into the furnace in an attempt to maintain the desired low pressure. This was not entirely successful, and the run was terminated early (after 19.5 hours - including heat-up) due to plugging of the furnace exhaust which was caused by sooting of the process gas.

TABLE 1. VACUUM DEPOSITION RUN NO. 18-14, DEPOSITION CONDITIONS

Case No.	Duration (hr)	Temperature Range (°F)	Pressure Range (mm Hg)	Gas Velocity ^a Range (ft/sec)	Total Gas Flow (SCFH)	N ₂ (volume percent)	CH ₄ (volume percent)	MTS (volume percent)
1	4.00	3220-3240 (1771-1782°C)	13-18	11.5-8.4	100	60	40	0
2	4.00	3280-3340 (1804-1838°C)	16-23	9.5-6.7	100	59.5	40	0.5
Adjusting gas flows and temperatures								
3	3.08	3360-3410 (1849-1877°C)	43-53	1.8-1.5	50	59.5	40	0.5
4	2.25	3480-3460 (1916-1904°C)	42-48	1.1-1.0	30	60	40	0

^aGas velocities assume ideality of gases and uniform heating of gases to deposition temperature.

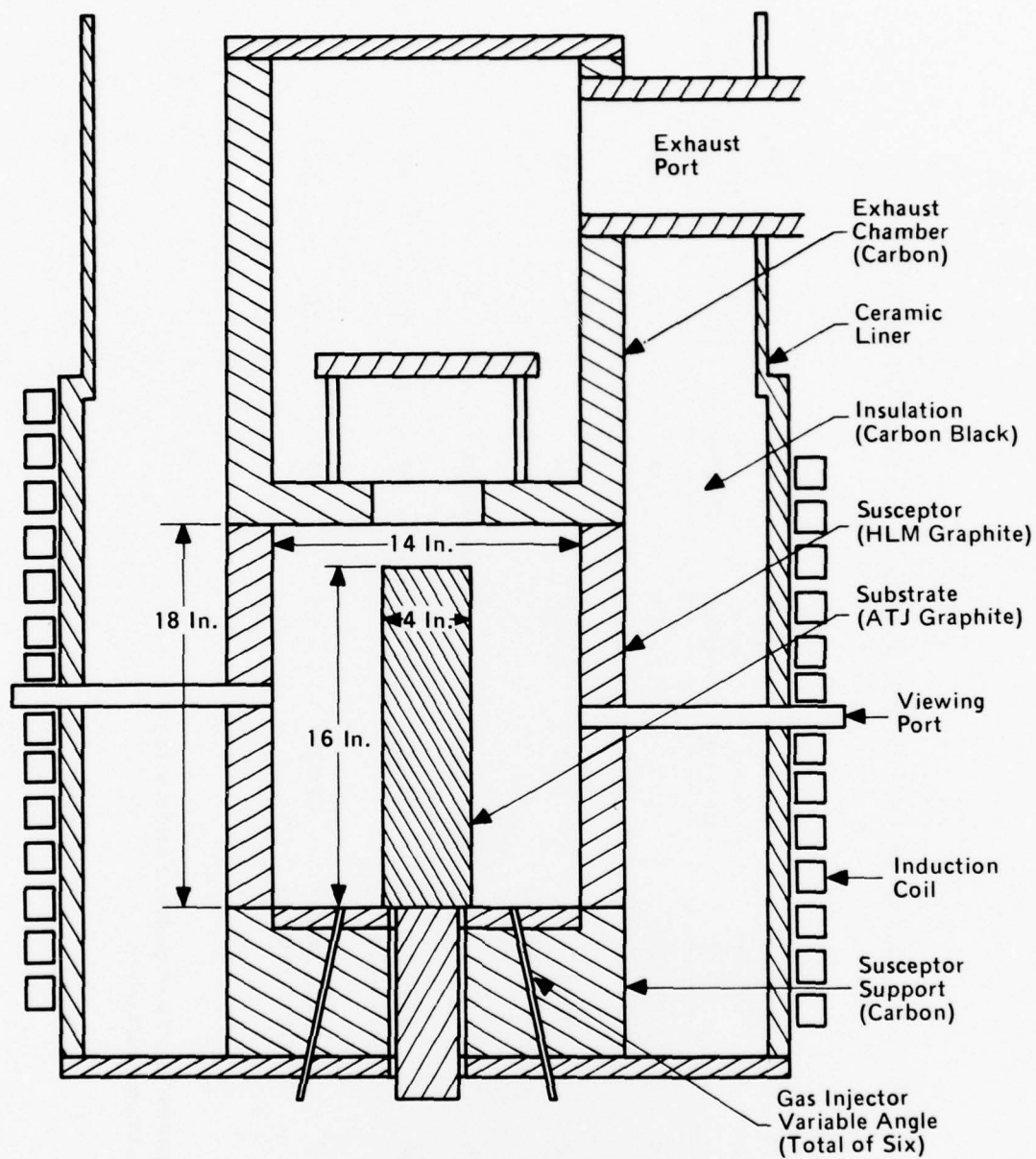


Figure 2. 18 Inch Vacuum Furnace (vacuum chamber not shown).

Silicon carbide needles were not present in the microstructure of either of the codeposited layers.

b. Run #18-15

The second coatings run of pyrolytic graphite codeposited with silicon carbide at reduced pressure was carried out in the same furnace as Run # 18-14.

This deposition (run 18-15) consisted essentially of three separate sets of process conditions. The first set of conditions deposited pure PG. This was used to provide a reference microstructure as well as a mandrel release coat. The second and third deposition layers were of PG/SiC codeposition.

The pyrolytic graphite was deposited from methane diluted with nitrogen. Codeposits of PG/SiC were deposited from methane and methyltrichlorosilane diluted with nitrogen.

The ranges of conditions for each test case are shown in Table 2. Deposition was performed on the outside of a cylindrical ATJ graphite substrate, 4 inches in diameter and 16 inches high. The geometry of the furnace deposition chamber is the same as used in Run # 18-14, shown in Figure 2.

A four-hour PG coating was initially deposited at $\sim 3800^{\circ}$ F on the substrate to permit release of the coatings from the mandrel as well as provide a reference microstructure. This PG deposition was conducted using a total gas flow of 150 SCFH, with methane comprising 40 volume percent of the total gas flow.

Between each of the deposition layers a flag or marker was deposited from undiluted methane for five minutes, followed by a purge of nitrogen for ten minutes.

During Case # 2, PG/SiC was deposited at a total gas flow of 100 SCFH, with methane comprising 40 volume percent and methyltrichlorosilane 0.9 volume percent. A furnace operating pressure of 12-13 mm Hg was scheduled, but during the run the pressure increased to 29 mm Hg. After 3 1/4 hours

TABLE 2. VACUUM DEPOSITION RUN NO. 18-15

Case No.	Duration (hr)	Temperature Range (°F)	Pressure Range (mm Hg)	Gas Velocity Range (ft/sec)	Total Gas Flow (SCFH)	N ₂ (volume percent)	CH ₄ (volume percent)	MTS (volume percent)
1	4.00	3780-3840 (2082-2116°C)	12-13	21.5-20.2	150	65	35	0
2	3.25	3155-3205 (1735-1763°C)	13-29	11.3-5.1	100	59.1	40	0.9
3	0.50	3260-3250 (1793-1788°C)	16	9.5-9.4	100	58.8	40	1.2

into the scheduled 4 hour deposition the run was terminated and corrective action attempted.

The vacuum valve to the furnace and all gas flows were closed. The vacuum filter element was then replaced with a new one and the filter re-assembled. This action reduced furnace pressure to 16 mm Hg and the next deposition (Case # 3) was started.

During Case # 3 PG/SiC was deposited at a total gas flow of 100 SCFH, with MTS comprising 1.2 volume percent of the total gas flow. After 30 minutes of deposition, with no rise in pressure, the process gases began exiting from the view tubes. This effect was initially thought to be due to clogging of the furnace exhaust tube. At this time the furnace operation was terminated, and a leak was found at the interface of the exhaust flange and the vacuum tank base. This leak was due to a faulty gasket.

Silicon carbide needles were not present in either of the co-deposition layers made during this run.

c. Run # 458-25

The third codeposition run of pyrolytic graphite and silicon carbide was performed in the 8 inch I.D. reduced pressure coatings furnace. The coating layers were applied to the outside of a stationary cylindrical graphite substrate 2 inches in diameter and 18 inches long.

Four sets of process parameters were tested in this deposition run to produce four PG/SiC codeposited layers. Between each layer a flag of pure PG was deposited from undiluted methane. The four layers of codeposited PG/SiC were the results of CVD using methane and MTS. No diluent nitrogen was used with the process gas during the deposition. Table 3. shows the range of conditions used during the four test cases.

Case # 1 and # 2 were performed under essentially identical conditions except for pressure. Case # 1 was performed at 5.5 mm Hg whereas Case # 2 was maintained at 30 mm Hg. A total gas flow of 10.6 SCFH was used of which MTS comprised 6 volume percent. Furnace temperatures were maintained from 3170° - 3290° F (1744° - 1810° C).

TABLE 3. VACUUM DEPOSITION RUN NO. 458-25

Case No.	Duration (hr)	Temperature Range (°F)	Pressure Range (mm Hg)	Gas Velocity Range (ft/sec)	Total Gas Flow (SCFH)	CH ₄ (volume percent)	MTS (volume percent)	Deposition Rate (mils/hr)
1	3	3220-3290 (1771-1810°C)	5.5	10.4-10.7	10.6	94	6	4.6
2	3	3250-3170 (1788-1743°C)	30.0	1.9	10.6	94	6	13.0
3	3	3050-3010 (1677-1654°C)	30.0	1.8	10.5	95	5	12.5
4	3	2970-3029 (1632-1660°C)	30.0	3.6	21.2	94	6	16.8

CH₄ 20 SCFH

MTS 8.25 oz/hr = 1.238 SCFH

N₂ 3

Case # 3 was performed at a reduced furnace temperature (3010°-3050° F). The difference between Case # 2 and Case # 3 was temperature, with Case # 2 run at ~ 3200° F and Case #3 at ~ 3000° F. Pressures and flow rates were essentially the same. A slight reduction in the MTS concentration from 6 to 5 volume percent resulted, in Case 3, due to temperature variance in the silane storage tank.

Case # 4 differed from Case # 3 in that the total gas flow was doubled. Temperature and furnace pressure were essentially unchanged.

The first set of conditions produced granular SiC crystals in the PG matrix. The remaining three cases deposited acicular (needle-like) SiC crystals in the matrix. Figure 3. contains photographs comparing the microstructures resulting from the four sets of process parameters.

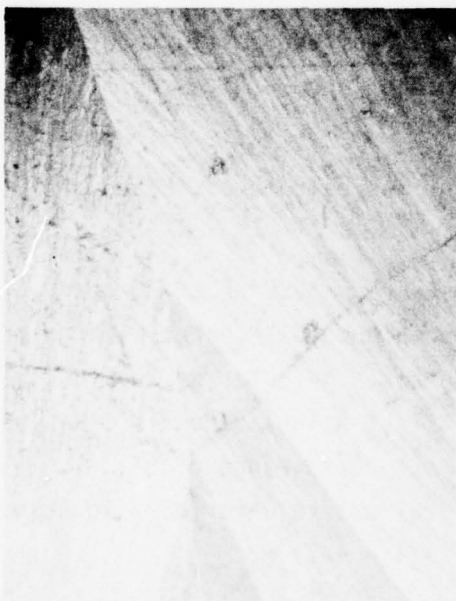
The coatings fabricated in this run were subjected to more detailed analysis than the coatings of the previous two runs. Following is a summary of the analysis of the coating microstructure of the four cases of run # 458-25. The results summarized below are outlined in Table 3.

Case No. 1: This test case was deposited at the highest furnace temperature (~ 3250° F) and lowest furnace pressure (5.5 torr) of the four cases. It was found to contain no SiC needles. Smooth, well-shaped PG cones (~ 30° angles) were observed. The initial 1/3 of the coating contained delaminations. The SiC concentration was determined to be 8.8% (sink/float method).

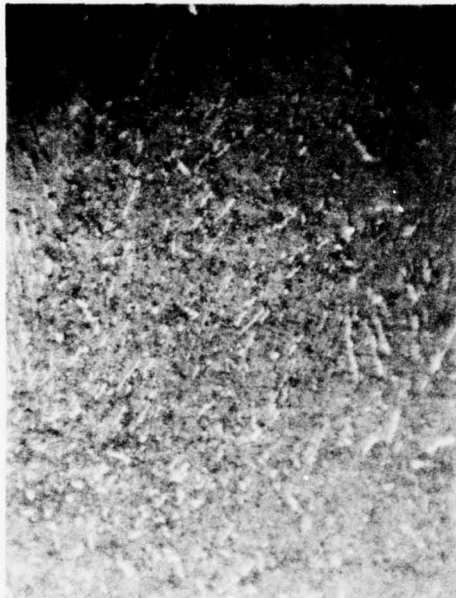
A deposition rate of ~ 4.6 mils/hr was calculated, based on the average coating thickness.

Case No. 2: The basic conditions were ~ 3200° F at 30 torr. The deposited cones were observed to be very smooth and well-shaped with good symmetry. Cone angles were found to be ~ 30 degrees. Acicular as well as asymmetrical SiC needles were present in the matrix. Acicular needle diameters range from .02 - .04 mils with an L/D aspect ratio range of 5/1 - 10/1. Some very large SiC crystals of asymmetrical nature were found to have average diameters of .06 mils and L/D ratios of 3/1 - 4/1.

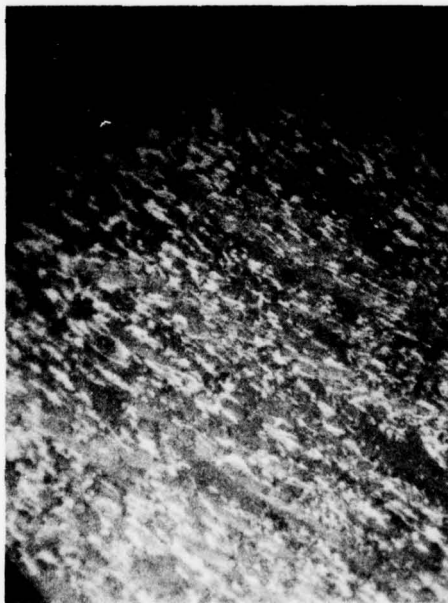
SiC distribution was very good in the PG matrix and consisted



Case-1 675X



Case-2 675X



Case-3 675X



Case-4 675X

Figure 3. Photomicrographs of Run 428-25 PG/SiC Depositions

TABLE 4. DEPOSITION RUN NO. 48-525

	Layer-1 (3250° F, 5.5 mm Hg)	Layer-2 (3200° F, 30 mm Hg)	Layer-3 (3025° F 30 mm Hg)	Layer-4 Douce Gas Flow (3000° F, 30 mm Hg)
SiC Content, weight percent	8.8	9.8	21.5	21.5
PG Cone Structure	Smooth	Smooth	Smooth	Smooth
PG Cone Angle	30°	30°	30°	30°
Delaminations	Yes	No	No	No
SiC Structure	None Noted	Acicular Needles - Asymmetric Crystals	Acicular Needles - Asymmetric Crystals	Acicular Needles - Asymmetric Crystals
SiC Distribution	—	Good	Good	Goof
SiC Diameter Mils	—	0.02 - 0.06	0.02 - 0.06	0.02 - 0.12
SiC L/D Ratio	—	3/1 - 10/1		4/1 - 20/1

of about 9.5 weight percent (sink/float method).

The average rate of PG/SiC deposition was ~ 13 mils/hr.

Case No. 3: Case No. 3 was deposited at $\sim 3000^\circ$ F (about 200° F lower than Case No. 2) at a pressure of 30 torr, and was found to contain smooth, well-rounded PG cones (30° angles) and SiC crystals. The SiC crystals were very evenly distributed and comprised about 21.5 percent of the matrix. Average needle diameters ranged from .02 - .06 mils with a few diameters of 0.4 mils. SiC crystals were found as acicular as well as asymmetrical shapes.

A deposition rate of 12.5 mils/hr was determined based on sample thickness.

Case No. 4: The temperature and pressure of this case were about the same as Case No. 3. The process gas flow rate was doubled. PG cone structures were found to be similar to those of the preceding three cases. SiC distribution was good and existed as interconnected asymmetrical shapes as well as acicular needles. Average SiC diameters varied from .015 to .12 mils with L/D ratios of 4/1 - 20/1. A silicon carbide content of ~ 21.5 was determined based on the sink/float density method. The deposition rate was 16.8 mils based on the average sample thickness.

d. Results Comparison

In the three runs comprising the parametric deposition experiments eleven combinations of temperature, pressure and gas flow rate were tested.

Dispersed silicon carbide aciculae were produced in three of the eleven cases. These coatings, Cases # 2, # 3, and # 4 of run # 458-25, were deposited at 2970 to 3250° F (1632 - 1788° C) with a furnace pressure of 30 torr from a process gas containing only methane and MTS. The MTS fraction was 5 to 6 volume percent.

The MTS volume percent and the furnace pressure appear as key parameters for forming SiC needles when deposited near the temperature of 3200° F (1760° C). Case # 1 of run # 453-25 was similar to cases # 2, # 3, and # 4 of that run except for having a lower furnace pressure (5.5 torr).

SiC was present in Case # 1, but no acicular structure was present.

The temperature dependence of SiC concentration was observed in run # 458-25 to be similar to that found when depositing PG/SiC at atmospheric pressure. Cases # 2 and # 3 which were performed under similar conditions except for temperature, show this relation. The 3250° - 3170°F (1788 - 1743° C) coating of case # 2 contained 9.8% SiC. The 3050° - 3010° F (1677 - 1654° C) coating of Case 3 contained 21.5 % SiC. By reducing the temperature from approximately 3200° F (1760° C) to 3000° F (1649° C) the SiC concentration was approximately doubled.

4. Coating Application Test - Run # 101-17

Run # 458-25 demonstrated that a dispersion of SiC aciculae could be grown within a PG matrix at subatmospheric pressure. This result suggested the possibility of modifying the basic codeposition process to operate at reduced pressure yielding significant benefits in terms of lower nitrogen consumption and elimination of the flow distribution problems encountered with complex geometries when depositing at atmospheric pressure.

With concurrence of the AFML Technical Monitor, the decision was made to direct the effort remaining on this program to determining the feasibility of reduced pressure codeposition for coating rocket nozzle components of realistic dimensions using a simulated half-scale entrance cap configuration.

a. Furnace Preparation

The 14 inch I.D. reduced pressure furnace required modification in two areas prior to this run: (1) Reduction and removal of excess soot expected to occur in the furnace exhaust and (2) installation of higher capacity MTS delivery and metering system.

(1) Residual Soot Removal

Previous experience with this furnace indicated that for this run a greater capability to remove or prevent the accumulation of soot in the vacuum line was necessary. Soot forms from excess process gases being heated to cracking temperature as they pass through the deposition and

exhaust chambers of the furnace. This soot is carried out through the exhaust line toward the vacuum pump. A filter in the line prevents the soot from reaching the pump. Under very sooty conditions, the filter will become restricted, which causes the furnace pressure to rise above desired levels.

Four methods of relieving the soot problem were recognized: (1) reduction of free volume in the deposition chamber (increasing the surface to volume ratio) allowing a reduction in the flow of process gases; (2) increased surface area in the exhaust chamber to deposit out greater amounts of carbon as PG/SiC rather than the low bulk density soot; (3) construction of a trap for the soot particles just outside the hot region of the furnace; and (4) installation of another filter in parallel with the existing vacuum line filter to allow alternate cleaning of one filter element while the other is in service.

The free volume of the deposition chamber was reduced by using a substrate larger than previously used in this furnace.

A series of stacked baffle plates was placed in the exhaust chamber to increase the surface area for deposition of PG/SiC from excess process gases, assuming that if more carbon is removed in the hot exhaust chamber as PG/SiC, less will be available to form soot which is carried out of the furnace by the gas flow.

A soot trap was built outside the furnace, but inside the reduced pressure chamber, to encourage settling out of the soot from the gas before flowing to the in-line parallel filters. The trap, shown in Figure 4, consisted of an 8 inch I.D. carbon pipe 48 inches high. The exhaust products entered the vertical pipe from a 6 inch I.D. carbon standpipe with open ports 12 inches from the bottom of the 8 inch pipe. The intent was for particulates to collect in the 12 inch high space at the bottom of the trap.

An in-line vacuum filter with twice the rated capacity of the existing filter was installed in parallel with the existing filter. A 3 inch diaphragm valve was attached to each end of each filter so that changing from one filter to the other could be accomplished smoothly. A mercury manometer was placed across the filters to indicate any changes in the differential pressure across the filter resulting from soot collecting on the element

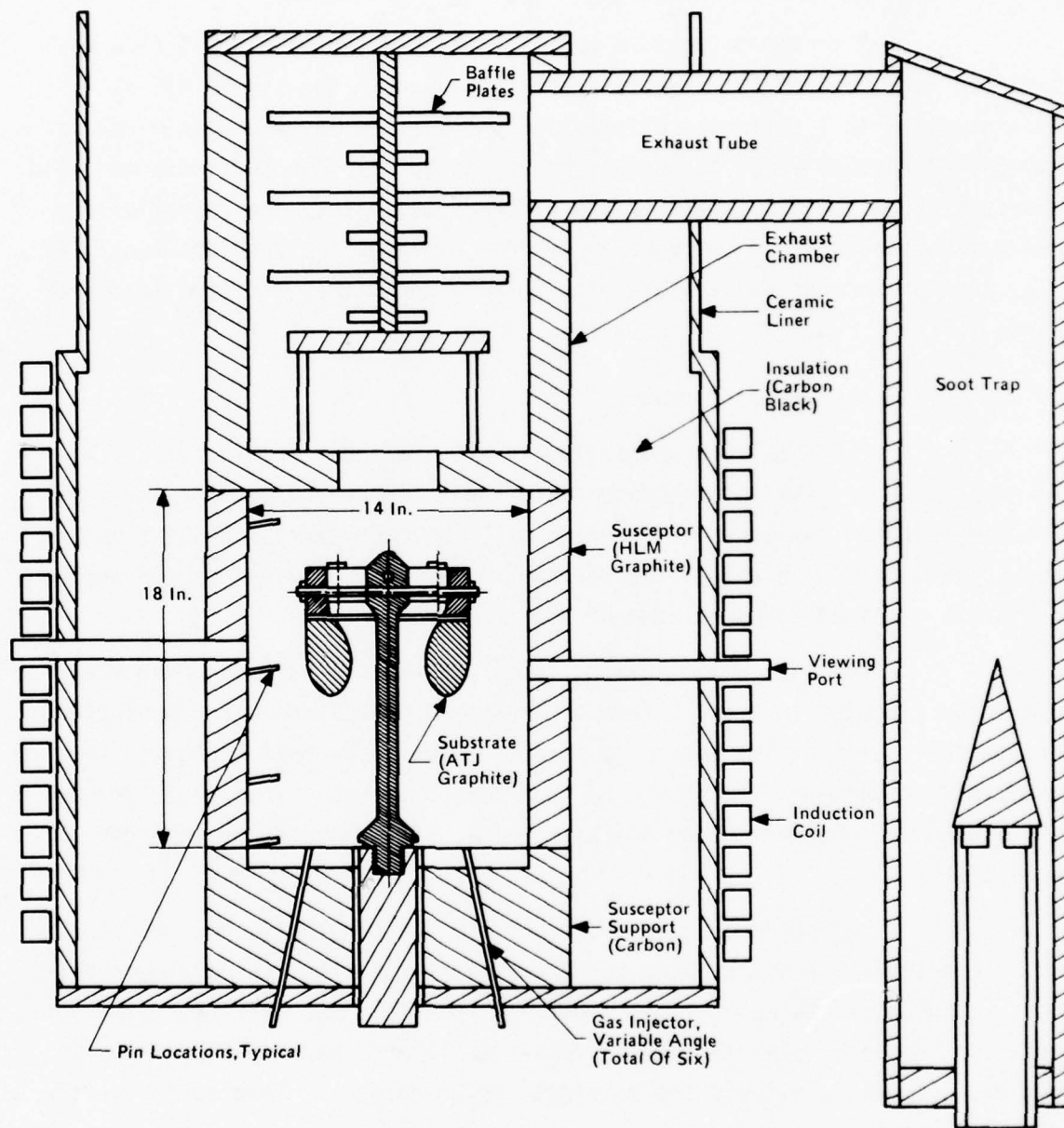


Figure 4. 14 Inch I.D. Reduced Pressure Furnace (vacuum chamber not shown).

and reducing gas flow through the filter. While one filter was in use, the other could be disassembled for cleaning of the element.

(2) Methyltrichlorosilane Liquid Delivery System

A system to deliver and accurately meter liquid MTS flow was assembled for use with the reduced pressure furnace. The liquid MTS flow was measured with a rotameter after which the MTS and methane were mixed as they passed through a 500 cc chamber heated to 80° C. The heat insured rapid vaporization of the MTS. This system offered reliability and repeatability that was not inherent in the bubbler system used with the previous runs. Also, the bubbler was not capable of supplying the higher MTS flow rates required for this run.

(3) Deposition Hardware

The substrate chosen for the run is shown in Figure 5. The ATJ graphite substrate was suspended with the entrance end down in the center of the deposition chamber. The process gas flow was upward, so the flow impinged on the entrance end of the nosecone surface before flowing both through the throat and around the outside of the substrate.

The suspension for the substrate was a 1 inch diameter graphite post which extended vertically from the bottom of the furnace and projected through the center of the substrate throat region. The post connected to a graphite ring above the substrate by four radial spokes. The substrate was fastened to the ring with four graphite bolts. See photographs in Figure 5. and 6.

During deposition the substrate was constantly rotated at 0.2 RPM. This speed was selected to approximate the rotation in the atmospheric pressure codeposit furnaces. The substrate rotation was imparted by the support post, which coupled to a drive mechanism located beneath the chamber. This mechanism also allowed the substrate to be raised or lowered for vertical alignment in the furnace.

b. Run Description

Run 101-17 was conducted at 3000° F (1649° C) within a pressure

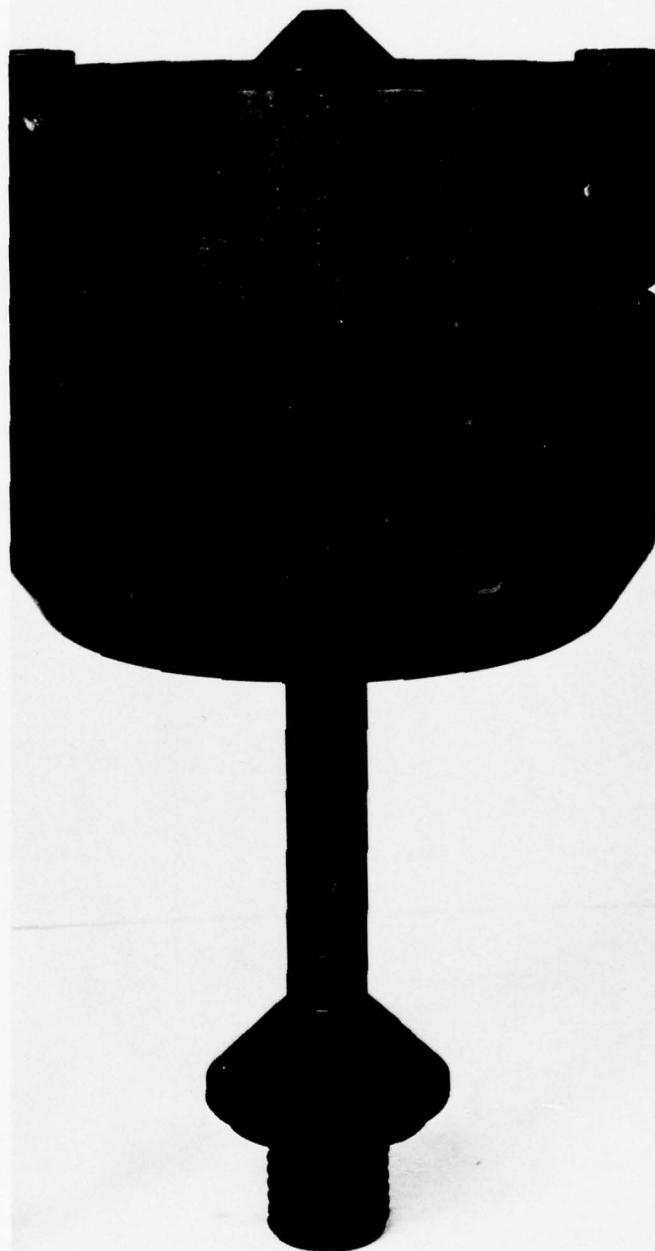


Figure 5. Run No. 101-17, Substrate and Support Assembly - Side View.

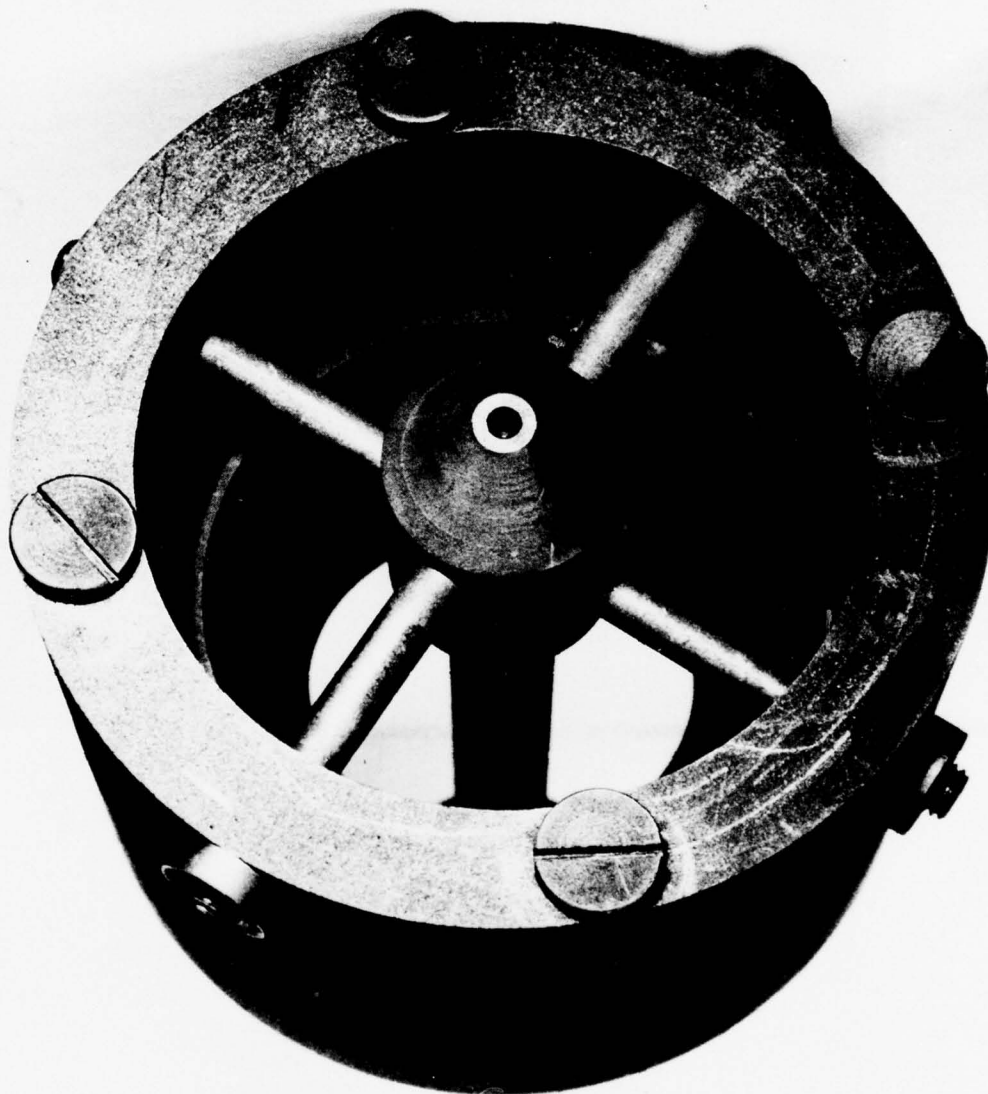


Figure 6. Run No. 101-17, Substrate and Support Assembly - Top View.

range of 14 to 23 mm Hg absolute. The PG/SiC CVD was from methane (94.3 volume percent) and methyltrichlorosilane (5.7 volume percent). The total process gas flow into the furnace was 100.7 SCFH (See Table 5.)

The target conditions for this run (3000° F, 15 torr, 94% CH₄, 6% MTS) were derived from the conditions of run # 458-25, case # 4. In that run, a 2 inch male mandrel was coated in a nominal 8 inch diameter furnace. The total gas flow rate for this run, which involved a much larger substrate and furnace, was established by scaling according to the ratio of flow areas, a factor of approximately five. The deposition temperature and gas composition were to be the same as during Run # 458-25, case # 4.

A lower pressure was chosen for this run in order to reduce the amount of sooting. It is known that the tendency for sooting increases as the volume of the deposition system increases. The maximum pressure at which sooting occurs is approximately inversely proportional to volume. Hence, the pressure chosen was one-half that of Run # 458-25, Case # 4, since the volume ratio for the two runs was approximately 2.

The intended operating pressure was 15 mm Hg; but during the run, as the inline vacuum filter collected soot, the furnace pressure increased due to the restricted flow. When a clean filter was brought in line, the pressure dropped back to the original value. The typical pressure pattern was a rise from 14 to 22 mm Hg over a 90-minute period followed by a drop from 22 to 14 mm Hg over a 1-minute period. There were five of these pressure fluctuations resulting from the five filter changes during the run.

The run was terminated after 8 hours of deposition. Soot film accumulation on the reduced pressure chamber windows prevented accurate temperature monitoring and dictated an early end to the run.

The exhaust chamber baffle plates and the soot trap which were to have removed the excess soot to prevent accumulation problems did not perform as planned. The baffle plates collected PG, as desired, but also caused turbulence and excessive gas heating in the exhaust chamber which resulted in sooting. Also, the soot particles that formed were too small to be settled out in the soot trap and were carried out of the chamber to collect in the vacuum lines as well as in the filters.

TABLE 5. DEPOSITION RUN NO. 101-17

Duration (hr)	Temperature (°F)	Pressure (torr)	Gas Velocity (ft/sec)	Total Gas Flow (SCFH)	CH ₄ (volume percent)	MTS (volume percent)	Deposition Rate (mils/hr)
8	2990-3055	14-23	12.5-7.8	100.7	94.3	5.7	7-18

c. Results

On the leading edge of the nose cap where the gas flow separated to flow around both the inside and outside of the substrate, a symmetrical feather-like skirt of PG/SiC developed, which grew into the gas flow at the point of separation. The skirt can be seen in the photograph of the coated substrate, Figure 7.

Several cracks in the coating originated on the outside surface of the substrate and, in two cases, propagated across the entrance end of the nose cap and continued about 1/2 inch into the inner portion. No coating cracks originated on the inside of the nose cap configuration. The coating was well bonded to the substrate, as evidenced by tensile failure of the ATJ graphite substrate, rather than debonding at crack sites in the coating.

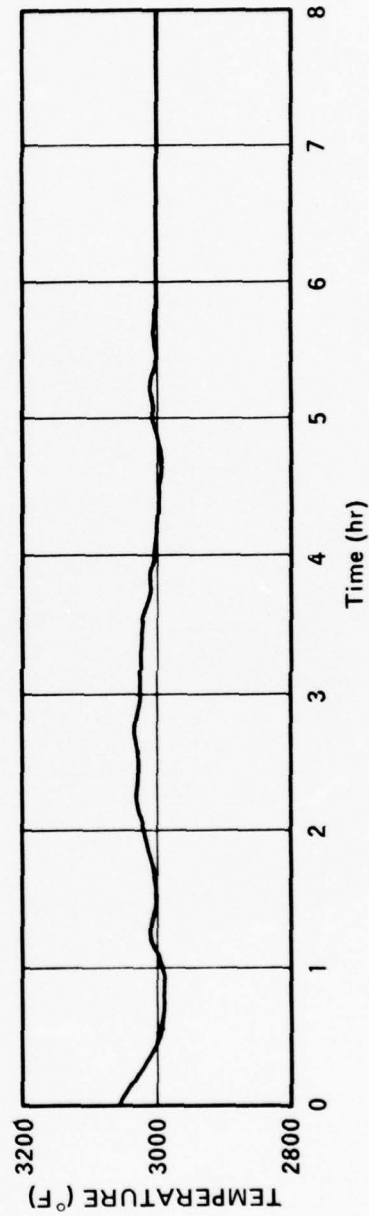
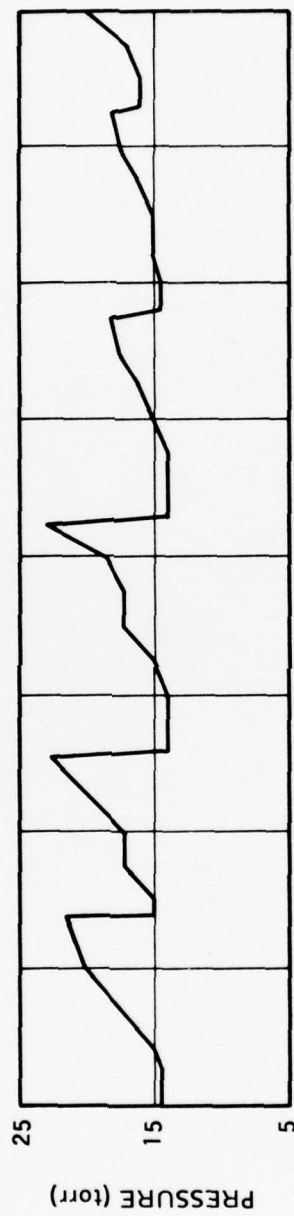
The PG/SiC coating varied in thickness from 0.058 to 0.150 inches with the thickest portions being farthest from the injectors. The silicon carbide in the PG matrix was present as acicular needles as well as asymmetrical grains. Five major microstructurally distinct bands developed in the coating which relate to changes in furnace pressure. Eighty to ninety smaller bands, evenly spaced across the coating, related to the rotation of the substrate during deposition and reflect asymmetry in the gas flow pattern. The bands can be identified in the photomicrograph montage of the entire coating thickness (Figure 8).

The five major bands, coincident with the five changes in furnace pressure, each had a SiC concentration gradient across the band. At position 2 on the subscale nose cap (See Figure 9), the SiC average concentration, as determined by electron microprobe analysis, increased from 5 weight percent at the beginning of a band to 20 weight percent at the end of a band. The average density at this position was 2.29. At position 3 (average density - 2.39), the SiC concentration increased across each band from 10 to 30 weight percent; and, at position 1 (average density - 2.13), the SiC concentration is related to the furnace pressure (which varied from 14 mm Hg at the beginning of a band to 22 mm Hg at the end of a band) and to the heating history of the deposition gases; that is, the duration and physical path of the gas from the injector orifice to the deposition surface.



Figure 7. Run No. 101-17, Substrate and Support Assembly - Coated.

Substrate-Coating Interface



75-1128-4

Figure 8. Run No. 101-17, Process Conditions and Photomicrograph Run No. 101-17, Magnification 70X.

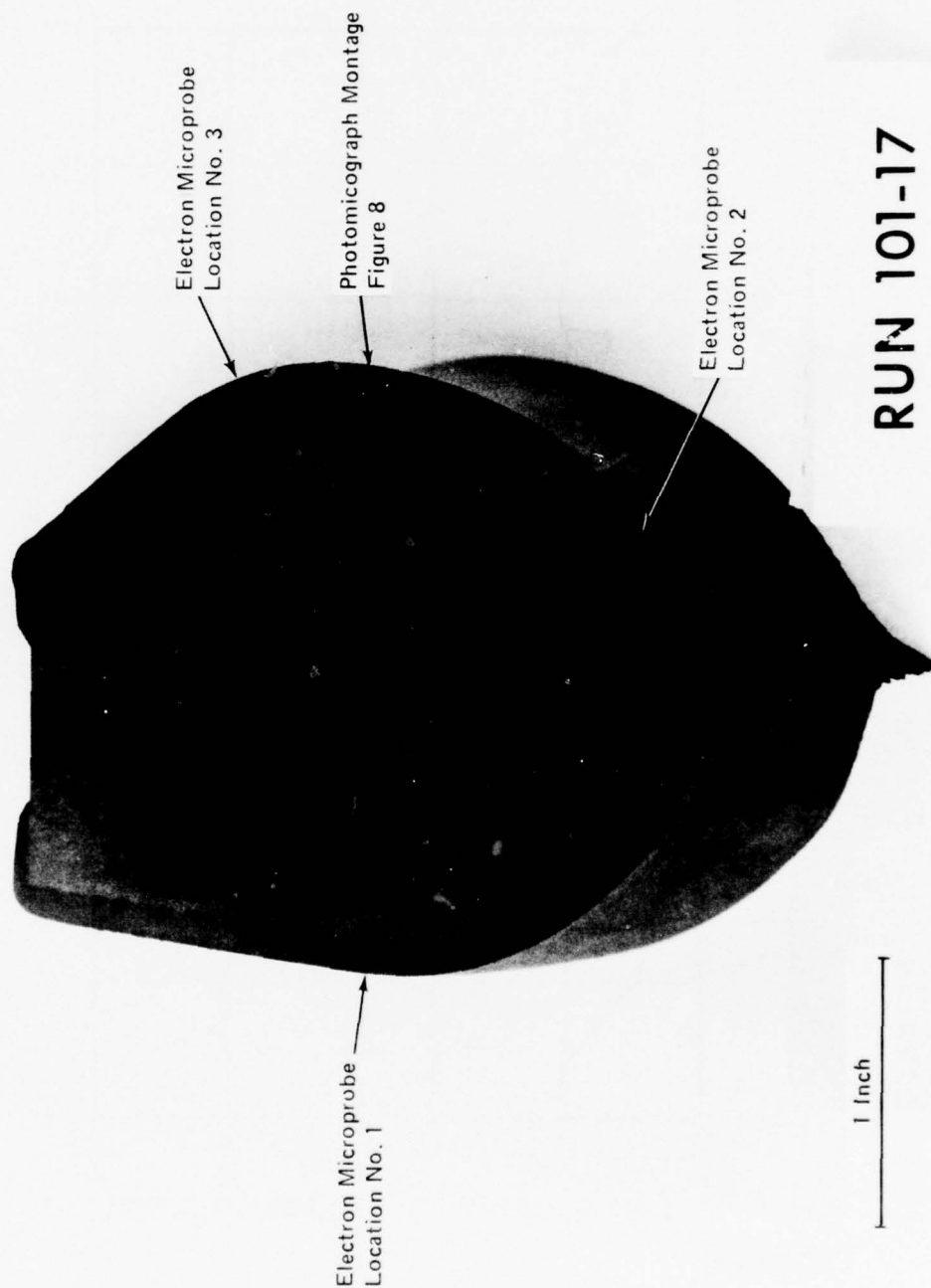


Figure 9. Run No. 101-17, Cross-Section of Coated Subscale Nosecap

Associated with any increase in the furnace pressure will be a corresponding decrease in gas velocity and an increase in residence time for gases which enter the deposition chamber at a constant mass flow rate. This may indicate that the increase in SiC concentration with increasing pressure was caused not by pressure alone, but by reduced gas velocity and increased time during which the deposition gases were heated before they reached the deposition surface.

Two other pressure related characteristics observed relate to the structure of the PG and the shape and size of the SiC crystals. As the pressure increased, the PG microstructure changed from a primarily surface nucleated to a primarily continuously renucleated structure. This change is most evident between 17 mm Hg and 19 mm Hg pressure. The SiC crystals (grains and aciculae) increased in size as the furnace pressure increased. Grains of SiC as large as 0.6 mil diameter were observed for pressures over 17 mm Hg, and the acicular shaped crystals showed an increase in L/D ratio from 2/1 at 18 mm Hg to 20/1 at 22 mm Hg with diameters in the range of .06 mil. The aciculae were oriented perpendicular to the deposition surface.

Each of the 90 minor bands (average thickness 1 mil) was composed of two layers: a layer of low SiC concentration followed by a layer of high SiC concentration. These low-to-high concentration differences vary from 15 - 20 weight percent to 5 - 40 weight percent, as determined by electron microprobe analysis. The low concentration layers had randomly distributed large SiC granules within the layers. The diameters of these granules averaged approximately one-half of the thickness of the layer with an occasional granule growing into a adjacent high concentration layer. The high concentration layers contained a web-like and fine granular SiC structure with the SiC well dispersed in the PG matrix.

The layering with the sharp increases and decreases in SiC concentration is attributed to asymmetry in the process gas flow, indicating the sensitivity of SiC concentration to changes in the flow patterns of the reactant gas mixture.

Stationary graphite pins 0.125 inch diameter and 2 inches long were located at four levels in the deposition chamber, spaced 45 degrees

apart and positioned at an 80 degree angle to the chamber wall to record gas flow phenomena during the run by the type, shape, and thickness of the coating deposited on each pin. The pin locations are shown in Figure 4. The coatings indicated reverse flow down the chamber walls with heavy recirculation on one side of the chamber. The recirculation caused excessive gas heating and subsequent sooting in part of the deposition chamber. This flow asymmetry was probably caused by the substrate and rotator mechanism being 1/4 inch off the center line of the deposition chamber and injector pattern.

SECTION IV FLOW ANALOG STUDIES

The PG/SiC codeposit furnaces normally consist of an annular channel into which process gases are fed by means of a multi-orifice injector. The flow passage is intended to be such that the gases are transported to the substrate to be coated while being heated to reaction temperature. The flow is nominally laminar ($N_{Re} < 2000$), but the jet momentum from the injector orifices is an important factor in determining the flow profile.

It has recently been recognized that the quality and quantity of the PG/SiC coating obtained may be significantly influenced by fluid dynamic phenomena. The optimum flow profile past the substrate is not currently known precisely. There are obvious interactions between flow phenomena and the thermal and chemical environment. One can also hypothesize transport mechanisms which could be heavily influenced by the nature of the flow past the part.

The importance of understanding how fluid dynamics may affect the deposition process is now recognized. To aid in obtaining this understanding, a two-dimensional flow simulator has been constructed. This unit has been operated to simulate the following coating configurations:

- Throat insert
- Conventional nose cap, single annulus
- Modified single annulus nose cap
- Double annulus nose cap
- Inverted nose cap.

The following discussion describes these tests and the conclusions resulting from these flow simulation studies.

1. Flow Simulator Design

The flow simulator was constructed of plexiglas to provide visual access to the flow passages. The unit is pictured in Figure 10. It represents a volume of above one-twelfth that of the codeposit furnace. The flow channel is full size, and the geometry is a cross section of the furnace from the injector to the exhaust port. The simulator is 14 inches long by 8 inches wide by 4 inches deep.

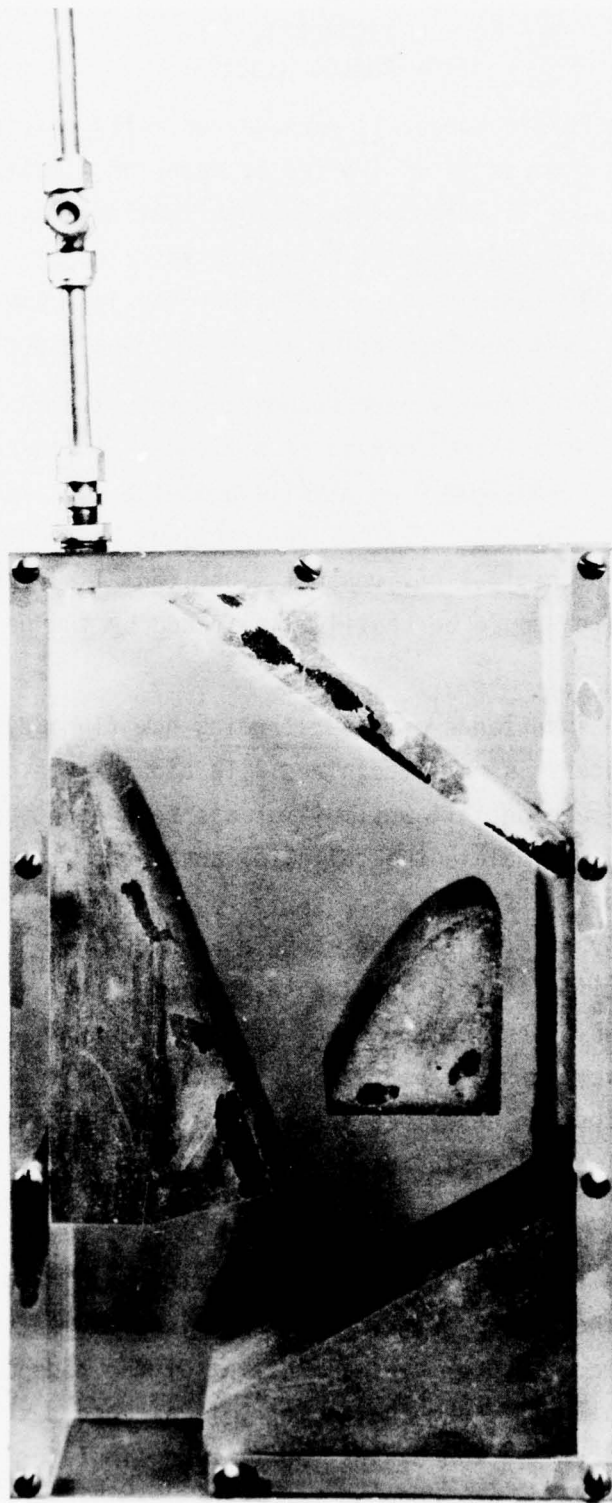


Figure 10. Flow Simulator in Double Annulus Configuration

The internal furnace components were simulated by bonding bulk graphite cutouts in place. The dimensions and spacing were identical to those used in actual furnace runs. An external connector was provided to permit installation of different injector configurations. Initial tests were made using N_2 gas as the fluid, with a bulk flow rate such that the Reynold's number was similar to that typical of furnace runs. Various types of smoke or particulate matter were injected into the gas stream as tracers of the flow profile. However, the flow variations were so rapid that they could not be followed with the naked eye. Consequently, a switch was made to water as the flow medium. The same Reynold's number simulation was maintained, but the linear velocity was reduced to the point where a dye tracer could be used to study the streamlines. The best results were obtained using a fuchsin red dye with a detergent solution added. The combination of dye and the small air bubbles allowed satisfactory study of cases ranging from laminar parallel flow to highly turbulent jet effects.

2. General Observations

Several surprising observations were made during the flow simulator studies. These may have a significant impact upon the design of flow passages and injectors in the future. The items noted below are general, and apply in varying degree to all configurations. Specific observations for the individual configurations will be discussed in detail later.

The first surprising observation was the degree of turbulence that can exist in a flow channel with a Reynold's number in the laminar region. The effect of the injector orifice jet momentum was clearly the dominant factor affecting flow in the upper part of the channel. In general, by the time the fluid medium passed the substrate, the flow was essentially laminar and parallel to the passage walls. This varied, of course, with the injector orifice size and orientation. On runs with a diffused injection pattern, flow was generally laminar and parallel throughout the simulator. However, the configuration that most closely simulated actual furnace operations exhibited extreme turbulence and serious flow perturbations because of the high momentum of the jet. The results of the high jet momentum varied depending upon the configuration tested.

A second general observation was that relatively minor changes in injector locations or orientation could result in major flow variations. This was particularly evident with the double annulus configuration shown in Figure 10. Movement of the injector vertically resulted in complete reversal of the flow direction around the part. Thus, the flow was bimodal and unstable. The impact of such flow variations in a deposition run could be immense. In other configurations, the effects were less pronounced, but still very significant, particularly when the flow channel diverged rapidly.

Another important observation was the effect of sudden changes in the flow geometry. Even with parallel laminar flow, a sudden divergence, step variation, or rapid turning of the flow could cause substantial recirculation. The effects of these recirculation zones, even near the base of the core body, could be seen to impact the flow in the vicinity of the substrate.

3. Throat Insert Configuration

Figure 11. shows the furnace configuration used successfully to coat throat inserts. This configuration was tested in the flow simulator to provide a basis for comparison with other designs. Table 6 lists the conditions tested in the simulator, and a brief statement of results.

The case which most closely resembles the actual furnace operation was a 1/8" injector orifice, oriented 45° to the axis and located so that the jet impinged near the center of the substrate. The Reynold's number based upon the wetted perimeter near the base of the substrate was about 1100. The flow simulator studies showed that the momentum of the jet was by far the dominant factor in determining the flow profile. In the case noted above, the jet impinged upon the substrate with a stagnation point near the center of the part. The flow recirculated back toward the roof and out toward the core. The turbulent identity of the jet was maintained to the base of the core, after which flow was generally laminar. The recirculation to the roof was static, in that the same basic element of fluid formed a vortex into which virtually no new fluid flowed. That is, an aerodynamic boundary existed which deflected the jet away from the roof and was driven by the aspirating effect of the jet itself. Conversely, the recirculation to the core was dynamic in nature. The flow formed a vortex, but the main body

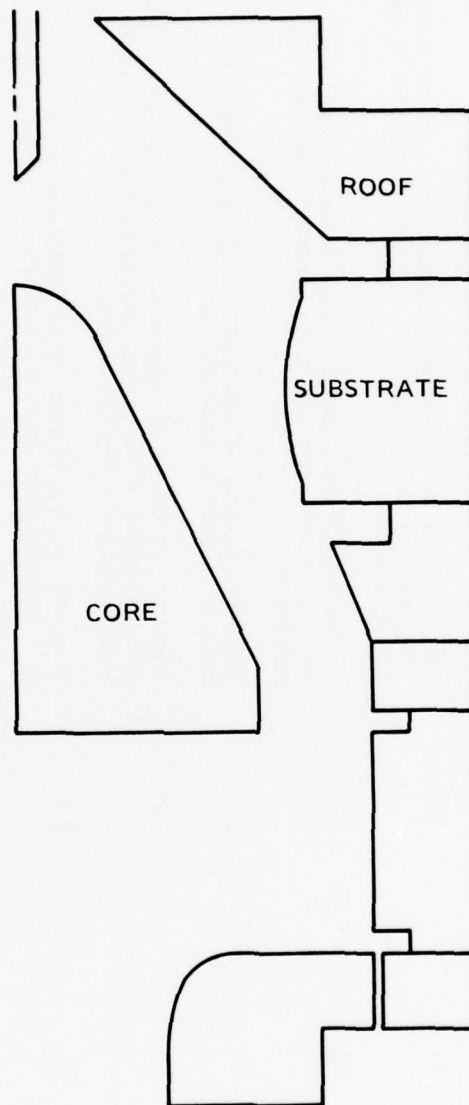


Figure 11. Internal Geometry for Throat Insert Deposition Runs

TABLE 6. THROAT INSERT CONFIGURATION

<u>N_{Re}</u>	<u>Orifice Size</u> <u>Inches</u>	<u>Orifice Angle</u> <u>Degrees from Axis</u>	<u>Distance</u> <u>from Core, in.</u>	<u>Results</u>
1100	1/8	45	0.5	Stag. pt. bottom of substrate; turbulence past core base; minimal recirc. to substrate and roof.
1100	1/8	45	1.5*	Stag. pt. upper center of substrate; recirc. to roof and core; turbulence to base of core.
1100	1/8	45	3.0	Stag. pt. top of substrate; extreme turbulence in upper slot; recirc. to core but not to roof; turbulence to base of substrate.
1100	1/8	60	2.5	Reflection off roof to core; turbulence in upper slot; recirc. between roof and core; turbulence to base of substrate.
1100	1/4	45	0.5	Stag. pt. at base of substrate; mild recirc to roof; mild turbulence to base of core.
1100	1/4	45	1.5	Stag. pt. at center of substrate; slight recirc. to roof; flow separates at base of substrate without recirc. in lower slot; turbulence to base of core.
1100	1/4	45	3.0	Stag. pt. at top of substrate; turbulence in upper slot, mild recirculation to core; turbulence to base of core.
1100	1/4	0	0.5	Flow attaches to core; slight recirc. to roof; mild turbulence in lower slot; mild turbulence to base of core.
1100	1/4	0	3.0	Flow attaches to core; very mild recirc. to roof and substrate; laminar below substrate.

* Nearest case to actual furnace operation.

continuously moved downstream and was replenished by the flow from the jet. The jet momentum was dissipated and the flow became laminar by the time it reached the base of the core.

Moving the injector location closer to the core moved the stagnation point further down toward the base of the substrate, with minimal change in the flow profile. However, relocating the injector near the roof resulted in significantly different flow characteristics. The fluid attached to the roof, and stagnated in the upper slot above the substrate. Recirculation of the dynamic type occurred out towards the roof, and turbulent flow persisted to the base of the substrate. This case resulted in all flow past the substrate going in the downstream direction with extreme turbulence in the upper slot.

Increasing the injector orientation angle from 45° to 60° resulted in impingement of the jet on the roof. The flow then reflected to the core, and there was general turbulence in the vicinity of the substrate, but with no direct impingement upon it.

The jet momentum was reduced by increasing the orifice size. This resulted in similar flow patterns to those noted above. The strength of the turbulence was greatly diminished, however. When the jet was directed down the axis to impinge on top of the core, the fluid attached to the core. Some jet separation occurred, resulting in moderate turbulence near the substrate. In general the flow was more laminar and parallel to the passage walls than in other cases.

4. Conventional Nose Cap Configuration

The single annulus configuration shown in Figure 12 has been used in most runs for coating nose cap substrates. This geometry results in direct impingement of the injector jet upon the substrate in a rapidly diverging flow channel. Results of flow simulator studies on this configuration are given in Table 7.

This flow geometry is characterized by a rapidly diverging channel to the substrate followed by sudden constriction at the base of the substrate. With the high momentum jet used in furnace operations, the flow

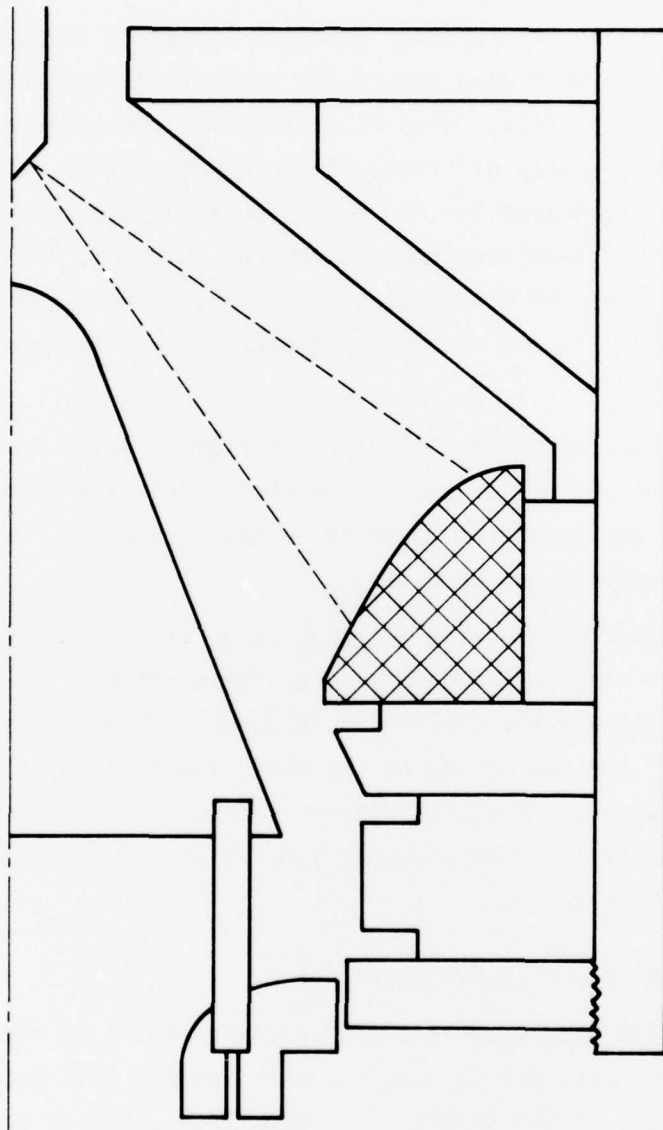


Figure 12. Internal Geometry for Single Annulus Nosecap Configuration

TABLE 7. CONVENTIONAL NOSECAP CONFIGURATION

N_{Re}	Orifice Size, Inches	Orifice Angle Degrees from Axis	Distance from Core, In.	Results
1100	1/8	45	0.5	Stag. pt. near base of substrate; recirc. to roof; turbulence past base of core.
1100	1/8	45	2.5*	Stag. pt. at upper center of substrate; recirc. to roof and core; turbulent to base of substrate.
1100	1/8	-45	2.5	Flow attached to core; recirc. to substrate and roof; turbulence to base of substrate.
1100	1/4	45	0.5	Stag. pt. near base of substrate; recirc. to roof; mild turbulence to base of substrate.
1100	1/4	45	2.5	Flow attached to roof; mild recirc. to core; mild turbulence to base of substrate.
1100	Porous	-	-	Parallel laminar flow; gentle recirc. between roof and core due to rapid channel divergence

* Nearest case to actual furnace operation.

impinges upon the substrate, then recirculates back to the roof and out to the core. The vortex formed near the roof is of the static variety. The net down flow of fluid continuously replenishes the core side vortex.

As in the insert case, the flow profile is dominated by injector jet effects. Moving the injector closer to the roof moves the stagnation point upwards, but the same basic pattern persists. If the orifice size is increased, the flow tends to attach to the roof, completely changing the flow character.

Dissipation of some of the jet momentum was accomplished by turning the injector 180° to splash against the wall. This resulted in attachment to the core with counterclockwise recirculation to the roof. The flow past the substrate in this case was upstream.

Total dissipation of the jet momentum was achieved using a porous diffuser. This led to parallel laminar flow, but with some mild eddy currents formed as a result of the rapid divergence of the flow channel.

5. Modified Single Annulus Nose Cap Configuration

The conventional nose cap geometry was modified to reduce the rate of channel divergence and provide smooth, large radius turns to direct the flow. The modified geometry is shown in Figure 13. The intent was to provide the maximum degree of laminarization of the flow before it reached the substrate. Results of these tests are given in Table 8.

In general, the modified design did result in laminarization of the flow. However, even in this geometry, the high jet momentum associated with the 1/8" injector orifices led to rather vigorous turbulence. The large radius turn tended to exhibit greater flow attachment (Coanda effect). The reduced divergence rate was still such that recirculation was not totally eliminated except with the porous injector.

6. Double Annulus Nose Cap Configuration

The double annulus geometry is intended to provide flow around the upper portion of the substrate, and thus insure sufficient coating thickness at this point in furnace runs. It is pictured in Figure 14.

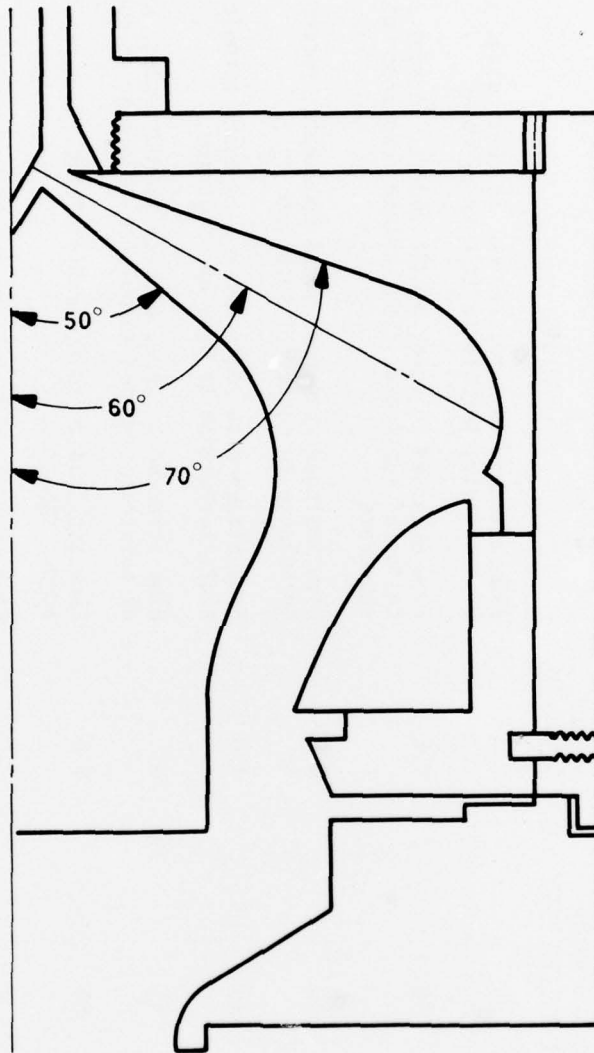


Figure 13. Modified Single Annulus Nosecap Configuration

TABLE 8. MODIFIED SINGLE ANNULUS NOSECAP CONFIGURATION

<u>N_{Re}</u>	<u>Orifice Size</u> <u>Inches</u>	<u>Orifice Angle</u> <u>Degrees from Axis</u>	<u>Distance</u> <u>from Core, In.</u>	<u>Results</u>
1100	1/8	45	0.5	Flow attached to core; recirc. to roof; stag. pt. at center of substrate; turbulence to base of core.
600	1/8	45	0.5	Flow attached to core; gentle recirc. to roof; stag. pt. at center of substrate, flow laminar downstream of center of substrate.
1100	1/8	60	0	Flow impinged upon roof above substrate; recirc. to core; turbulence to center of substrate.
1100	1/8	60	1.0	Flow attached to roof; recirc. to core; turbulence in upper slot; turbulence to base of substrate.
1100	1/4	60	0	Flow attached to core; recirc. to roof; stag. pt. near top of substrate; gentle turbulence to center of substrate.
1100	1/4	60	1.0	Flow attached to roof; gentle recirc. to core; flow laminar across substrate.
1100	Porous	-	-	Flow laminar, parallel to wall throughout channel.

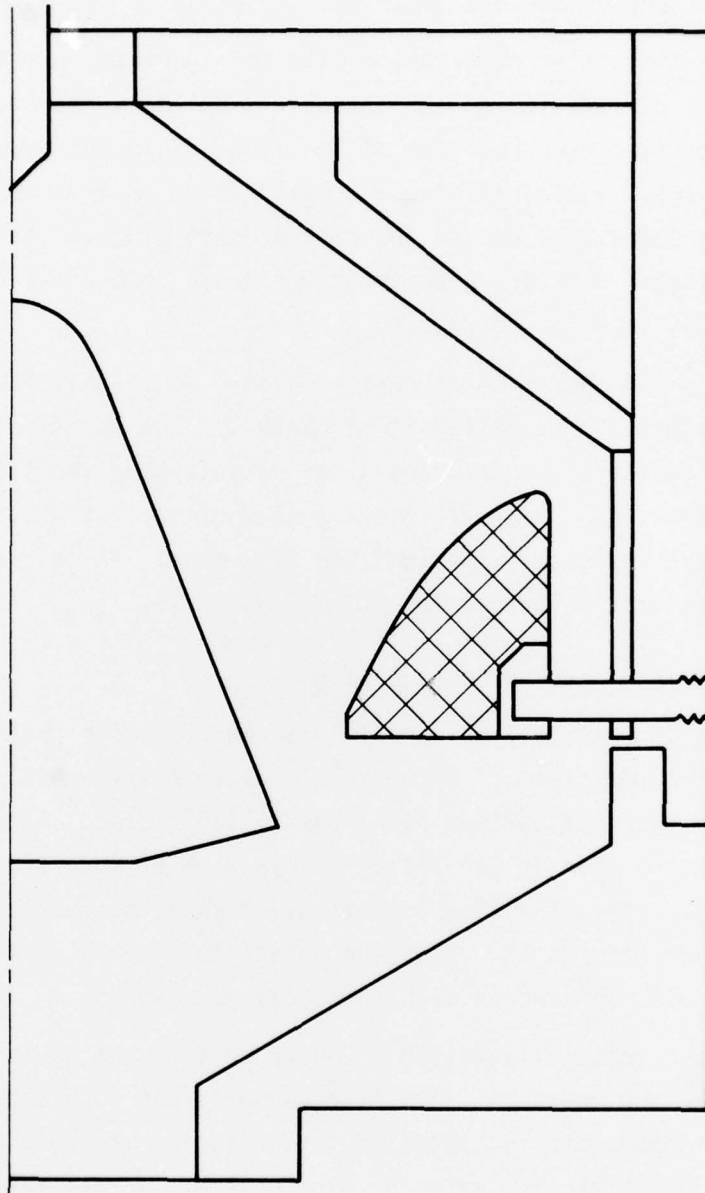


Figure 14. Double Annulus Nosecap Configuration

Results of the flow simulator tests on this configuration are given in Table 9. A photography of one dye experiment is shown in Figure 15.

The surprising observation with this geometry was the bimodal nature of the flow. Relocation of the injector vertically resulted in either clockwise or counterclockwise rotation of the flow around the substrate. If located very precisely, a stagnation point would exist on the substrate, and flow would proceed downstream around the part on both sides. This balance was extremely delicate, however, A slight upset could change the flow from split to rotational, in either direction.

This configuration appears to be the most sensitive to injection parameters, and the most difficult to control. The normal growth of coating thickness could result in substantial variation of the flow profile. However, with a porous injector with the momentum of the jet dissipated, flow becomes laminar and proportional to the flow area. In this case, flow is stable and downstream on both sides of the substrate.

7. Inverted Substrate Nosecap Configuration

The desirability of parallel laminar flow for coating operations has not been demonstrated. From a fluid dynamic standpoint, however, this appears to be the most definable and controllable case. Figure 16 represents an attempt to provide parallel, laminar flow by inverting the substrate. In this geometry, the flow channel divergence is minimized, as is the need to turn the flow as it passes the substrate. Table 10 lists the results of flow simulator studies with this configuration.

These tests illustrated the need to turn the fluid gently, if turbulence is to be avoided. The core base geometry was such that the flow could not stay attached. It separated and stagnated on the wall opposite the core base. This led to recirculation of flow upstream across the substrate, at times covering two-thirds of the substrate surface. This observation led to modification of the core geometry to be used in actual furnace runs.

As noted before, the orifice jet momentum plays a dominant role in determining flow character. The 1/8" orifice cases generally retained the identity of the jet down to the substrate, and the turbulence

TABLE 9. DOUBLE ANNULUS NOSECAP CONFIGURATION

N_{Re}	Orifice Size Inches	Orifice Angle Degrees from Axis	Distance from Core, In.	Results
1100	1/8	35	1.5	Stag. pt. at center of substrate; flow counterclockwise around substrate; turbulence to base of core.
1100	1/8	75	2.5	Flow attached to roof; flow clockwise around substrate; recirc. zone between substrate and core.
1100	1/4	35	2.5	Mildly turbulent flow clockwise around substrate.
1100	1/4	35	1.5	Stag. pt. at center of substrate; flow downstream on both sides of substrate.
1100	1/4	35	0.5	Flow attached to core; mildly turbulent flow counterclockwise around substrate.
1100	Porous	-	-	Flow laminar; proportional to flow area; downstream on both sides of substrate.

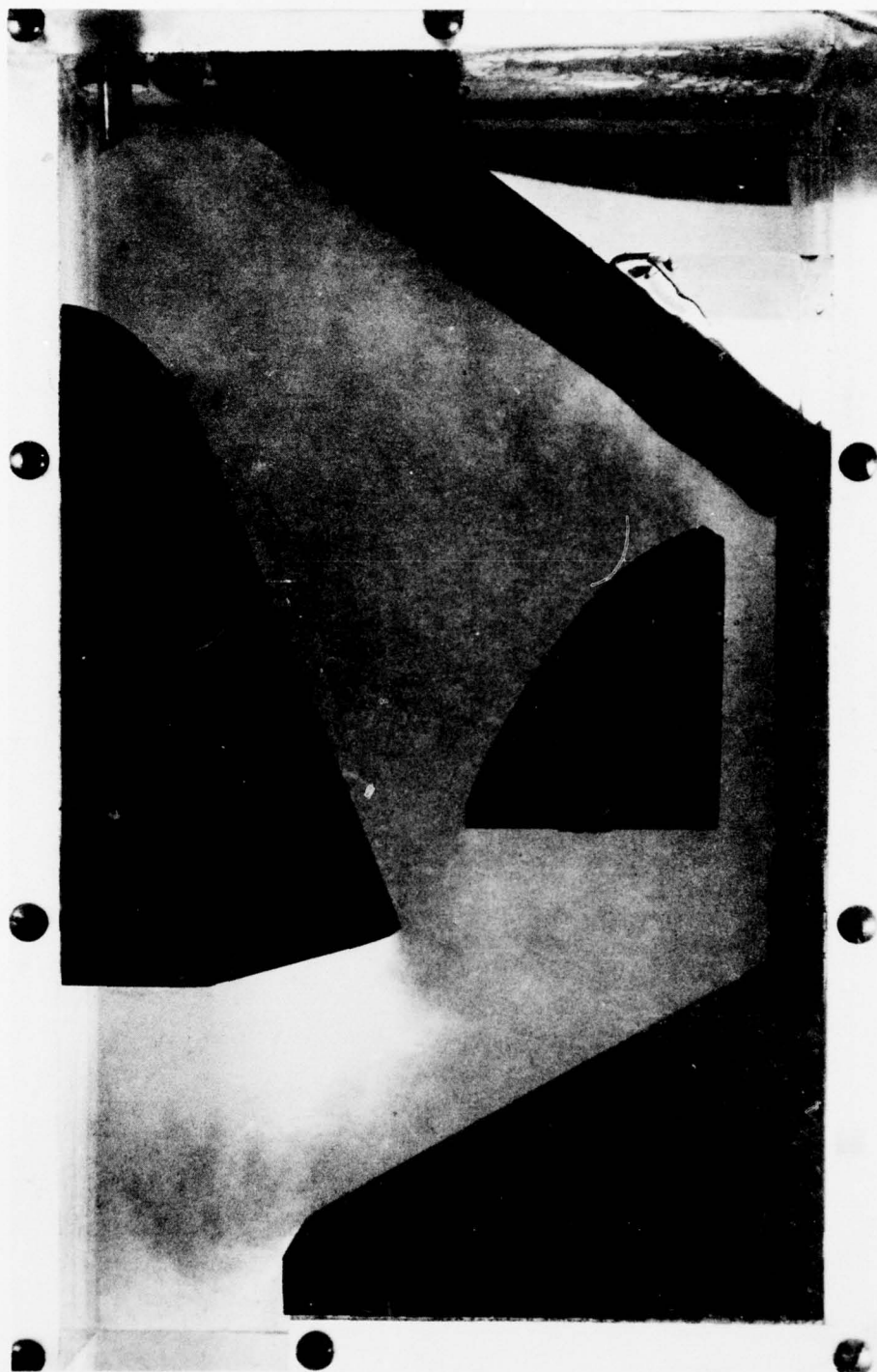


Figure 15. Typical Dye Injection Flow Test
of Double Annulus Configuration.

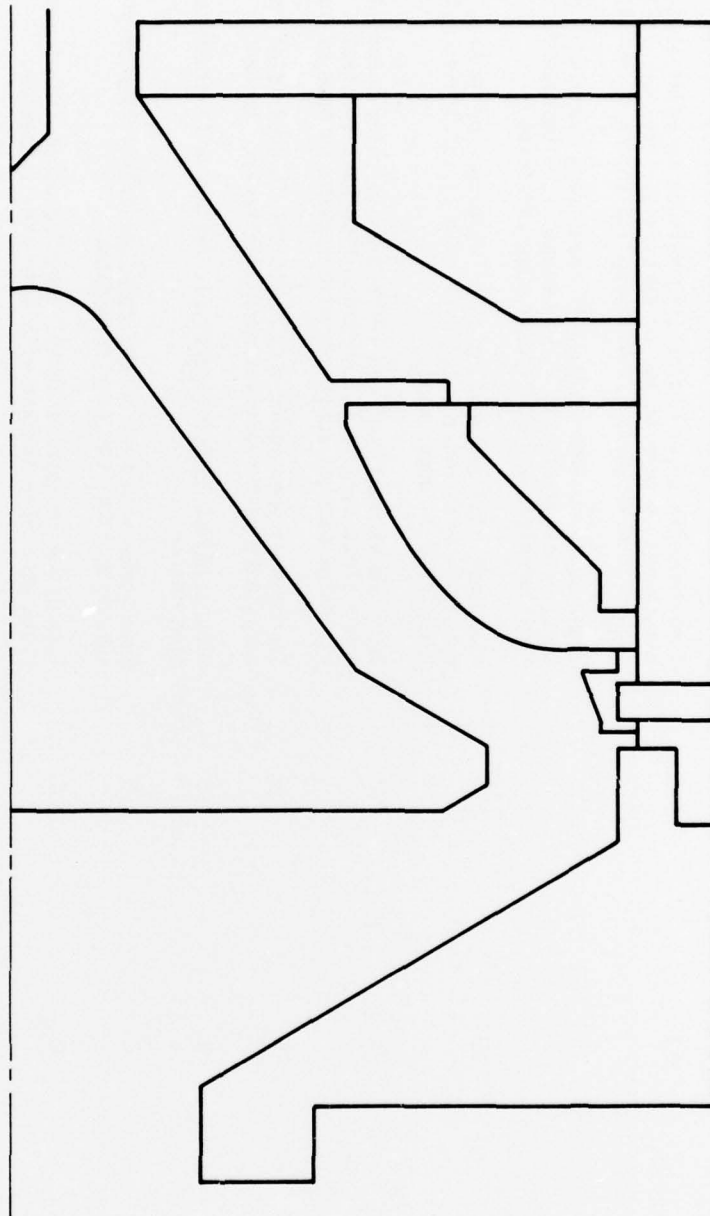


Figure 16. Internal Geometry for Flow Tests of Inverted Substrate Nosecap Configuration

TABLE 10. INVERTED NOSECAP CONFIGURATION

N_{Re}	Orifice Size Inches	Orifice Angle Degrees from Axis	Distance from Core, In.	Results
600	1/8	45	2.5	Flow impinged upon roof, reflected to core; gentle turbulence to center of substrate; stag. pt. below base of substrate with recirc. to lower half of substrate.
1100	1/8	45	2.5	Turbulence in upper channel; turbulence in upper slot; attachment to core at top of substrate; stag. pt. below substrate with recirc. causing upflow to top of substrate.
1600	1/8	45	2.5	Vigorous turbulence to base of core; very turbulent in upper slot; momentum effects strong enough to eliminate recirc.; flow turbulent and downstream past substrate.
600	1/8	45	0.5	Flow reflected off roof to core; stag. pt. below base of substrate with recirc. to lower half of substrate; mild turbulence in upper slot.
1100	1/8	45	0.5	Impingement upon roof and reflection to core; turbulence in upper slot; turbulent downstream flow past substrate; stag. pt. below base of substrate with recirc. to base of substrate.
1600	1/8	45	0.5	Impingement upon roof; very turbulent in upper slot; general turbulence past substrate overcomes recirc. tendency.
600	1/4	0	2.5	Flow attached to core; parallel, laminar with minor separation eddies.
1100	1/4	0	2.5	Some turbulence near top of core; generally laminar past substrate with some eddy formation.
1600	1/4	0	2.5	Turbulence in upper channel; eddy formed on lip of upper slot; generally laminar with some eddy formation.

created could be observed to the base of the core. It is apparent that the jet momentum must be low in order to achieve parallel, laminar flow which can be analytically defined.

8. Injector Criteria

The flow simulator studies have shown clearly the importance of the injector in establishing the flow profile in the codeposit furnaces. The small orifice jets currently used impose a high degree of turbulence into a nominally laminar flow system. The bulk N_{Re} in the furnaces is only 1,000 - 1,500 at the zone of least flow area. The jet often exhibits N_{Re} of 35,000 to 50,000 and exit velocities up to 500 ft/sec. Thus, the entire flow system is dominated by the jet influence. The presence of static recirculation zones in some geometries makes analysis of the flow complex, as the aerodynamic boundaries formed result in incomplete filling of the flow volume.

From a fluid dynamic standpoint, the obvious solution is a low or zero momentum injection system. However, the total answer is not that simple. The interactions of the flow parameters with the thermal and chemical environments must also be considered. Laminar flow might change the rate of heating of the gas, as well as its residence time, before reaching the substrate. The impact of these interactions is yet to be defined.

The current discrete orifice injector design also requires rotation of the furnace canister to average out flow perturbations and assure a uniform part. As would be expected, when the unit is not rotated, the injector pattern can be seen clearly on the coated part. There are several ways in which this effect could be remedied. The use of porous or transpiration injectors would certainly result in homogenous flow. Other possibilities are impinging element injectors, slots, or the introduction of swirl or rotation to the injected gases. However, the most desirable injector configuration cannot be designed until more information is available concerning the above-mentioned interactions.

9. Conclusions from Flow Simulation Studies

The major contribution of the flow simulator studies to date is recognition of the dominance of the injector in establishing the flow

profile. Even though the bulk flow is well into the laminar region, even at the most constricted flow area zones, the jet turbulence is so great that turbulent eddies can often be observed well past the substrate location.

Other flow perturbations can be induced by rapid divergence of the flow channel or sudden turning of the flow direction. These factors are minor compared to the injector effects, but can lead to unexpected recirculation areas or stagnation points where they may not be desirable.

The double annulus configuration is the least stable from a fluid dynamic standpoint. This geometry can exhibit bimodal flow characteristics in which the flow can recirculate around the substrate in either direction, or bifurcate at the substrate and pass around both sides in the downstream direction.

It is clear that laminar, parallel flow can be imposed upon any of the geometries considered by a combination of reduced jet momentum and improved flow passage design. However, the desirability of parallel, laminar flow has not yet been proven. This type of flow would maximize controllability and be relatively simple to model analytically. Therefore, if it is compatible with the other parameters such as the thermal profile, the gas concentration, and the transport properties, it could represent a significant improvement in understanding of the codeposit process.

SECTION V CONCLUSIONS AND RECOMMENDATIONS

The major conclusions drawn from the experimental results of this program are:

- (1) An acicular SiC structure can be obtained in a PG/SiC coating deposited at reduced (subatmospheric) pressure.
- (2) The SiC structure is related to pressure.
- (3) Acceptable deposition rates can be achieved when codepositing at reduced pressure.
- (4) Reduced pressure codeposits bond strongly to ATJ substrates.
- (5) Smooth coatings can be achieved at reduced pressure when the gas flow is parallel to the coating surface.

It is recommended that additional deposition experiments be conducted in order to define the envelop bounded by pressure, temperature and gas composition in which the acicular SiC structure occurs. Such data will be needed before optimized process conditions can be defined. These data should be supplemented with analyses (and experiments as necessary) to quantitatively describe flow patterns and heat transfer mechanisms in the deposition furnace.